

Acoustic-Gravity Waves in the Thermosphere of Venus

ANTHONY D. DEL GENIO¹ AND GERALD SCHUBERT

Department of Earth and Space Sciences, University of California, Los Angeles, California 90024

AND

JOE M. STRAUS

*Space Sciences Laboratory, The Ivan A. Getting Laboratories, The Aerospace Corporation, P.O. Box 92957
Los Angeles, California 90009*

Received November 13, 1978; revised April 24, 1979

Properties of acoustic-gravity waves in the upper atmosphere of Venus are studied using a two-fluid model which includes the effects of wave-induced diffusion in a diffusively separated atmosphere. In conjunction with neutral mass spectrometer data from the Pioneer Venus orbiter, the theory should provide information on the distribution of wave sources in the Venus upper atmosphere. Observed wave structure in species density measurements should generally have periods ≈ 30 – 35 min, small N_2 , CO, and O amplitudes, and highly variable phase shifts relative to CO_2 . A near resonance may exist between downward phase-propagating internal gravity and diffusion waves near the 165-km level at periods near 29 min. As a result, if very large He wave amplitudes are observed near this level, it will indicate that the wave source is below the 150- to 175-km level and that the exospheric temperature is close to 350°K. Wave energy dissipation may be an important mechanism for heating of the nightside Venus thermosphere. Large-density oscillations in stratospheric cloud layer constituents are also possible and may be detectable by the Pioneer Venus large probe neutral mass spectrometer.

INTRODUCTION

In comparison with the terrestrial thermosphere, very little is known about the chemistry, structure, and dynamics of the upper atmosphere of Venus. The height of the Venus turbopause, for example, was unknown until the first direct density measurements of neutral nonreactive species above 100-km altitude were made by the Pioneer Venus bus neutral mass spectrometer; preliminary results suggest an altitude of ~ 137 km (von Zahn *et al.*, 1979).

Another unknown is the Venus dayside exospheric temperature. Early ionospheric models and Mariner 5 Lyman- α hydrogen scale heights suggested an exosphere at 700°K (McElroy, 1969). However, Mariner 10 uv spectrometer hydrogen scale heights (Broadfoot *et al.*, 1974) and helium airglow

data (Kumar and Broadfoot, 1975) are consistent with a temperature of 375–400°K. Early Pioneer Venus data seem to support a low value, but discrepancies among the first results of several different experiments (cf. Niemann *et al.*, 1979; von Zahn *et al.*, 1979) leave open the question of temporal as well as spatial variability. As a result, the profile of solar energy deposition by euv radiation is still uncertain.

Likewise, little was known prior to Pioneer Venus about the nature, magnitude, and distribution of energy deposition by the solar wind. Venus may have a small intrinsic magnetic field, but it is not strong enough to hold off the solar wind, which must therefore interact directly with the ionosphere (Russell *et al.*, 1979). Whatever the nature of this interaction, we would expect it to produce a distribution of thermospheric heat sources radically different from that found on Earth.

¹ Present address: NASA Goddard Institute for Space Studies, New York, N. Y. 10025.

Much information about the state of an atmosphere can be revealed by studying the properties of acoustic-gravity waves which propagate in that atmosphere. The Pioneer Venus orbiter mission provides an excellent opportunity for identifying thermospheric waves on Venus. The orbiter carries a neutral mass spectrometer (ONMS) which measures the number densities of neutral constituents at altitudes of ~ 150 – 500 km (Colin and Hunten, 1977). The maximum average vertical spacing (~ 400 m at 500-km altitude) and horizontal spacing (~ 2 km along the satellite path) of sample points are sufficient to resolve the important scale sizes of any wavelike density variations which may occur at these levels during the 8 months of the nominal mission. Considering the wealth of wave phenomena which are known to occur in the Earth's upper atmosphere (Hines, 1960) and the lower stratosphere of Venus (Belton *et al.*, 1976), the chances for wave detection in the thermosphere of Venus at some time during the Pioneer Venus orbiter mission would appear to be excellent.

Mass spectrometers aboard the Earth-orbiting AE-C satellite (Reber *et al.*, 1975; Potter *et al.*, 1976) have already recorded wavelike density variations at thermospheric levels which Dudis and Reber (1976) and Del Genio *et al.* (1978, 1979) have interpreted as internal gravity waves. The amplitudes and phases of density oscillations vary from species to species in the thermosphere because of the different scale heights of the various gases in this diffusively separated region. When wave-induced diffusion has time to operate, though, amplitude and phase differences disappear. This change of behavior with wave period makes it possible to place limits on the propagation characteristics of observed waves.

In this paper we apply the theory of acoustic-gravity wave propagation in a diffusively separated atmosphere, with wave-induced diffusion included (Del Genio *et al.*, 1978, 1979), to waves in the upper atmo-

sphere of Venus. By comparing the results with ONMS observations of constituent density responses to gravity wave passage during the Pioneer Venus mission, it will be possible to identify the most common periods, wavelengths, phase speeds, and propagation directions of acoustic-gravity waves in the Venus thermosphere. This in turn should help us to learn more about the spatial and temporal distribution of heat sources at high altitudes on Venus.

THEORY

The mathematical model is that developed by Del Genio *et al.* (1978, 1979) for terrestrial waves. The atmosphere consists of two neutral ideal gases with basic state density profiles characteristic of diffusive equilibrium. The background is hydrostatic and has an isothermal temperature profile which is the same for the two constituents. Background winds are neglected; unless large thermospheric wind shears exist, a horizontal wind component parallel to the wave propagation direction would merely Doppler shift the wave frequency. All forms of dissipation other than wave-induced diffusion (viscosity, heat conduction, ion drag, etc.) are also neglected. These mechanisms are certainly important in determining the total dissipation of wave energy in the thermosphere and their effects in this regard will be briefly discussed. However, they should be of secondary importance in determining species phase and amplitude differences compared to the direct collisional coupling between individual gases.

Collisional coupling is taken into account via terms representing the collisional transfer of momentum and thermal energy between species. There are two characteristic time scales related to interspecies collisions which affect upper atmospheric wave motions. The first is the mean collision time for a molecule of the minor species with any molecule of the major species, which increases with altitude, due to the decreasing density and attendant longer mean free paths. When this mean collision time be-

comes comparable to the wave period, the validity of the continuum hypothesis and the assumption of Maxwellian velocity distributions break down.

The second relevant time scale is the characteristic diffusion time for a minor species through the major gas,

$$\tau_{\text{diff}} = L^2/D_{st}, \quad (1)$$

where L is a characteristic length scale and D_{st} is an appropriate diffusion coefficient for two species s and t . Two different diffusion times can be defined. For vertical diffusion, we might take $L = H_p$, the pressure scale height of the atmosphere, while for horizontal diffusion, an appropriate choice might be $L = 1/\alpha = \lambda_x/2\pi$, where α and λ_x are the horizontal wave number and wavelength, respectively, of the wave. If the wave period is comparable to or greater than either of these two diffusion times, wave-induced diffusion of at least one kind will be important.

On Venus, collision and diffusion times vary more sharply with altitude in the lower thermosphere than on Earth, because of the small scale height of the heavy major constituent on Venus, CO_2 . Consequently, only in the lowest parts of the Venus thermosphere are the mean collision times short enough to justify the use of continuum theory and Maxwellian distributions for time-dependent atmospheric motions. For example, if we use the Venus ionospheric model of Kumar and Hunten (1974), which assumes a dayside exospheric temperature of 350°K , and divide each constituent density by e to shift densities by one scale height and obtain better agreement with the observed ionospheric peak (Hunten, private communication), we find that at 175-km altitude, mean collision times are <10 sec, while vertical diffusion times are ~ 0.5 – 2 min. Since time scales at least an order of magnitude greater than mean collision times are desirable when using continuum theory, this is probably the highest altitude that should be discussed when considering typical acoustic-gravity waves. At 150 km, the

diffusion times for He, O, and N_2 through CO_2 are ~ 24 , 55, and 85 min, respectively, and consequently, some interesting diffusion effects will occur at intermediate and long periods. At these altitudes, since CO_2 scale heights are so small, horizontal diffusion will be important only for $\lambda_x \leq 50$ – 75 km. Of course, given the uncertainty in the composition and structure of the upper atmosphere of Venus, these collision and diffusion times are probably reliable only to within a factor of 2 or 3.

When constant collision frequencies are assumed and the plane wave assumption is made in the horizontal and time coordinates, as was done in Del Genio *et al.* (1978, 1979), the governing equations define an eigenvalue problem with four possible roots of the characteristic equation. Two of these roots represent a pair of upgoing and downgoing acoustic-gravity waves modified by wave-induced diffusion. However, in a two-component fluid, there are two additional roots corresponding to highly damped waves with very small vertical wavelengths and phase and amplitude relationships which, in the terrestrial case, are inconsistent with all satellite observations of wave properties. These "diffusion waves" are of little interest in most cases on Earth because of their extreme damping, and in general, the same should be true on Venus. Therefore, in the following section, we will concentrate mainly on acoustic-gravity modes, which are the most likely to be detected by Pioneer Venus. There is one instance, though, in which diffusion waves may be significant on Venus and this will also be discussed.

PHASE AND AMPLITUDE RELATIONSHIPS

To illustrate the effects of wave-induced diffusion, we first consider waves at 150-km altitude on Venus with $\lambda_x = 400$ km. At this level, CO_2 is taken to be the major species, and O, He, and N_2 are in turn taken to be the minor species. CO, which has the same molecular weight as N_2 , should exhibit

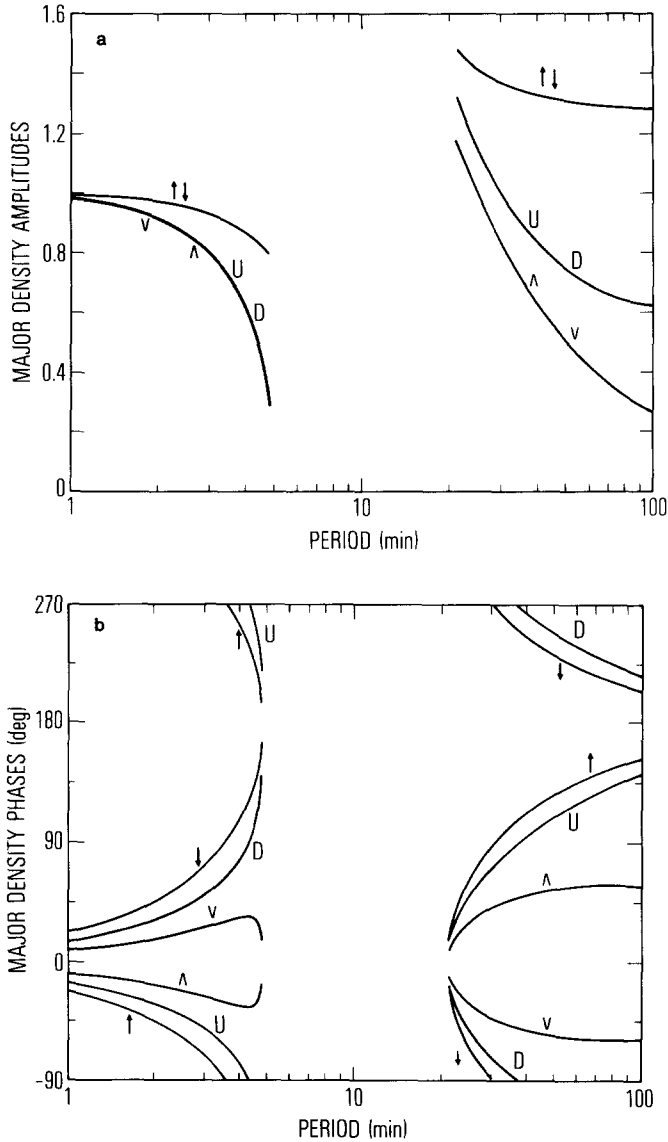


FIG. 1. Fractional density (a) amplitude ratios and (b) phase differences for acoustic-gravity waves at 150-km altitude on Venus for $\lambda_x = 400$ km and K_{gr} 10^{10} times its actual value at 150 km. U and D refer to O-CO₂ amplitude ratios and phase differences for waves with upward and downward phase propagation, respectively; Λ and v are the corresponding quantities for N₂-CO₂, while \uparrow and \downarrow refer to He-CO₂.

characteristics very similar to N₂, unless substantial photochemical effects exist.

For most of our calculations, we use the 350°K exospheric temperature model of Kumar and Hunten (1974), with the densities divided by e , for our constituent densities, and the low euv efficiency model of Dickinson and Ridley (1977) for the details

of the Venusian temperature profile. Effective collision radii σ for He-CO₂ and N₂-CO₂ are derived from an extensive survey of experimentally determined diffusion coefficients (Mason and Marrero, 1970); σ for O-CO₂, which is not included in that survey, is estimated as 3.2×10^{-8} cm in the 150- to 175-km altitude range on the basis of

a rough interpolation of the values of σ for He-CO₂ and N₂-CO₂. Amplitude ratios and phase differences for the density perturbations are given by the magnitude and phase angle of the complex ratio of the fractional density fluctuations of the two gases.

In the limit of infinite collision frequencies (i.e., infinite diffusion times), velocity and temperature differences between species vanish and the atmosphere moves like a single-component fluid. Figure 1 shows amplitude ratios and phase differences as functions of wave period when the collision frequencies are taken to be 10¹⁰ times their realistic values at 150-km altitude. The two branches of these curves represent acoustic waves (short periods) and internal gravity waves (long periods); the region in between contains only evanescent waves, which are generally not of interest except at interfaces and boundaries in an atmosphere.

It can immediately be seen that upgoing (with respect to phase propagation) and downgoing waves have identical amplitude ratios and mirror image (about either 0 or 180°) phase differences. Very near the evanescent region, wave properties vary sharply with period and, in fact, depend on the particular basic state chosen. At other periods, though, the behavior approaches asymptotic limits. In the short-period acoustic limit, all amplitude and phase differences vanish. In the long-period internal gravity wave limit, though, the amplitude ratio for each constituent pair approaches a different constant value: 0.6 for O-CO₂, 1.3 for He-CO₂, and 0.1 for N₂-CO₂. These numbers will vary somewhat with the altitude and basic state chosen, but the qualitative result—large He amplitudes and small O and N₂ amplitudes relative to CO₂—will not change. Furthermore, in this same limit, the phase difference approaches 180° for O-CO₂ and He-CO₂. For N₂-CO₂, the phase difference is sensitive to the altitude and basic state being considered and may vary considerably from case to case.

Amplitude and phase differences arise

because density perturbations are the result of two competing effects in the continuity equation, adiabatic expansion and vertical advection. For heavy gases like CO₂ with small scale heights, vertical advection dominates and density perturbations are in phase with the vertical velocity. For light gases (He, O), though, density gradients are small and the divergence term dominates; density perturbations are then out of phase with both the vertical velocity and the density perturbations of the heavier gases. The greater the dominance of one term or the other, the larger the amplitude of the density fluctuation will be. For intermediate molecular weights like that of N₂, the two effects almost cancel; N₂ amplitudes will thus be small and the phase difference between N₂ and the heavier CO₂ may be large or small, depending on how the balance between the two terms tips for a given basic state and altitude.

When we include diffusion, though, the situation changes dramatically. Figure 2 shows amplitude ratios and phase differences for the same case, but with realistic values of the collision frequencies at 150-km altitude. One obvious effect of diffusion is that amplitude and phase relationships are now somewhat different for upgoing and downgoing waves; this is most likely due to the vertical anisotropy introduced by diffusion via its interaction with the vertically varying background density profiles. The other difference between Figs. 1 and 2 is that at long periods, amplitude and phase differences tend to disappear when diffusion is taken into account. The decrease begins at wave periods comparable to the vertical diffusion times for the gases. This occurs because diffusion acts to offset the differences created by the mass-dependent background density profiles of the individual gases. For heavy gases, molecules diffuse out of the disturbed fluid parcel to counteract the large advection contribution, and for light gases, molecules diffuse into the parcel to increase the relatively low concentration of light gases in-

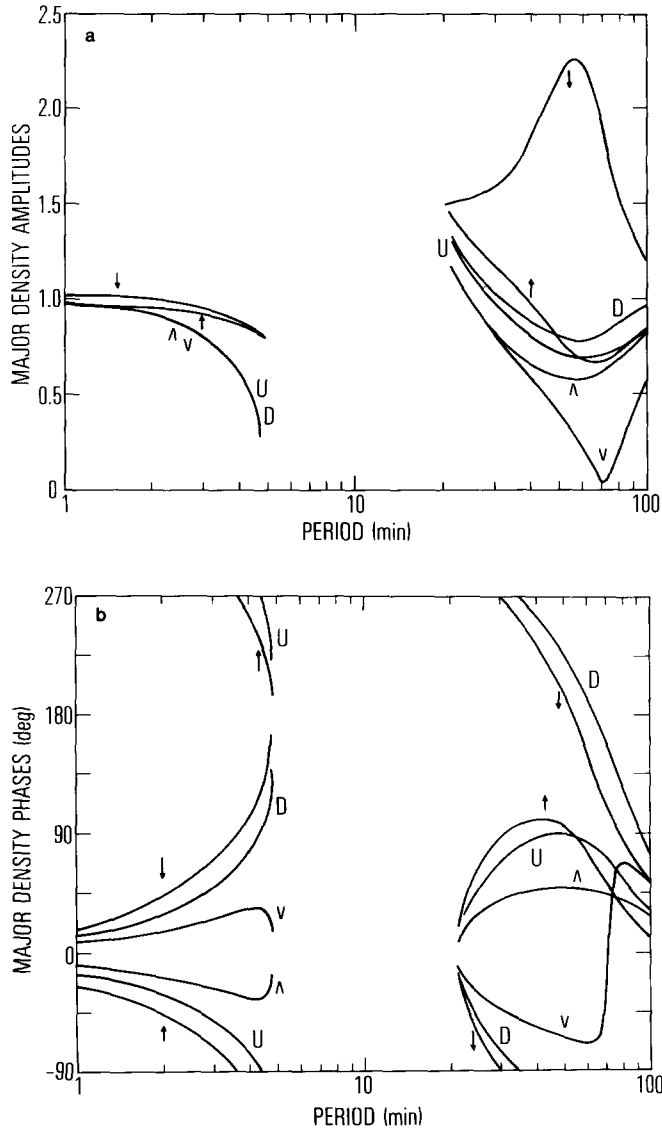


FIG. 2. The same quantities as plotted in Fig. 1, but for a realistic K_{st} .

side the parcel. The elimination of amplitude and phase differences does not set in until long periods because, at shorter periods, diffusion does not have sufficient time to operate.

In general, at short periods, the behavior is similar to that which occurs when diffusion is neglected. The He-CO₂ amplitude ratio is an exception to this rule; at intermediate internal gravity wave periods, it de-

viates substantially from the behavior predicted by Fig. 1 and also from that expected on the basis of the discussion in the preceding paragraph. This deviation becomes even stronger at higher altitudes. Figure 3 shows acoustic-gravity amplitude and phase relationships for a 400-km wave at 165-km altitude. At this and higher altitudes, CO₂ is no longer the single dominant species. For calculations at the 165-km and 175-km

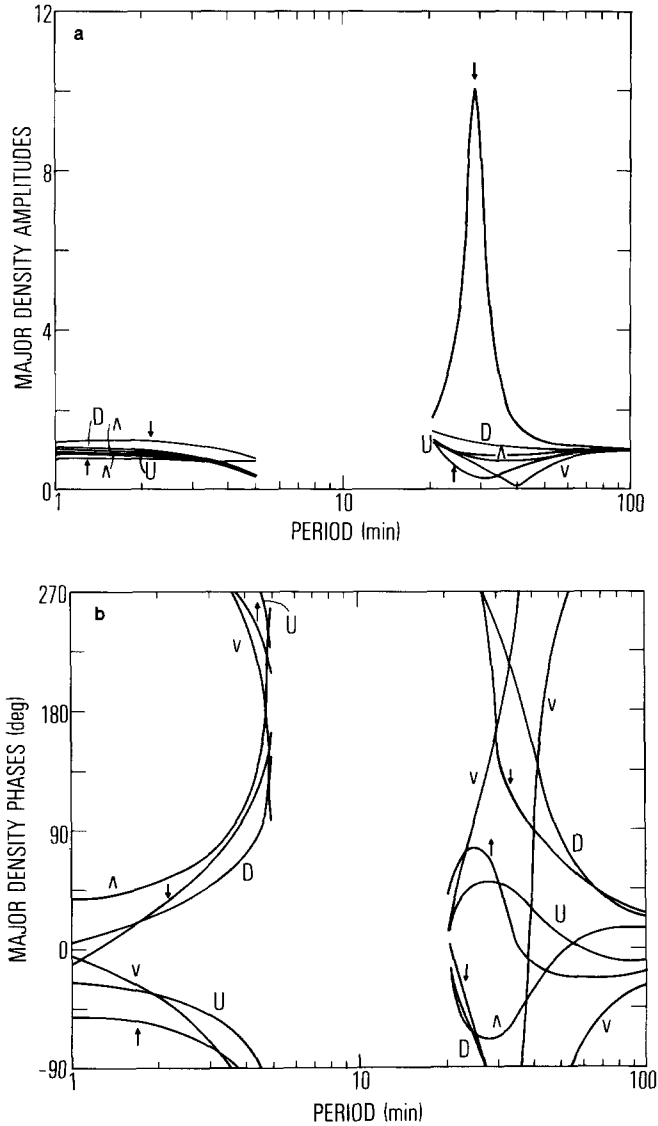


FIG. 3. The same quantities as plotted in the previous figure, but for $\lambda_x = 400$ km at 165-km altitude.

levels, therefore, we take the major "species" to be a mixture of O and CO_2 for use in the He and N_2 models. For the O model, of course, CO_2 alone remains the major species. To obtain He- CO_2 and N_2 - CO_2 amplitude and phase differences, we now must compare density fluctuation ratios from the He and N_2 models with a corresponding ratio from the O model [see Eqs. 15 and 16 of Del Genio *et al.* (1979)].

O- CO_2 amplitude ratios and phase differences are calculated as before.

Diffusion effects are apparent at shorter periods in Fig. 3 because of the decreasing diffusion time accompanying an increase in altitude. The most interesting aspect of this figure is the sharp peak in the He- CO_2 amplitude ratio for a downgoing wave at ~ 29 min period. At this period, the vertical wavelengths of the downgoing acoustic-

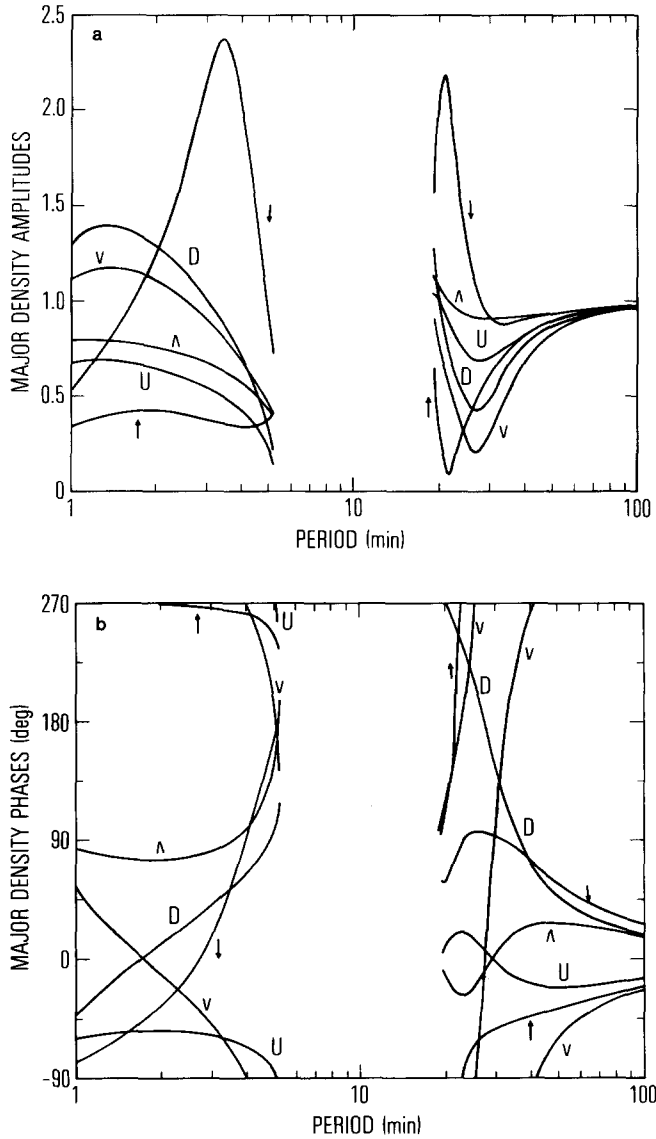


FIG. 4. The same quantities as plotted in the previous figure, but for $\lambda_x = 400$ km at 175-km altitude.

gravity and diffusion modes become equal, while the real part of the vertical wavenumbers for the two waves differ by only $\sim 16\%$. What seems to be occurring at this level, therefore, is a near resonance between the downgoing acoustic-gravity and diffusion waves. An acoustic-gravity wave propagating into this region with the appropriate period and horizontal wavelength would thus resonantly excite a corresponding diffusion wave.

The possibility of this type of resonance has been investigated for the terrestrial thermosphere by Gross and Eun (1976), who suggested that whenever the complex vertical wavenumbers of any two of the four possible modes are equal, the density response of the minor constituent becomes infinitely large. Internal gravity and diffusion waves are tightly coupled at resonance, so the total response will be determined by a linear combination of both modes, not one

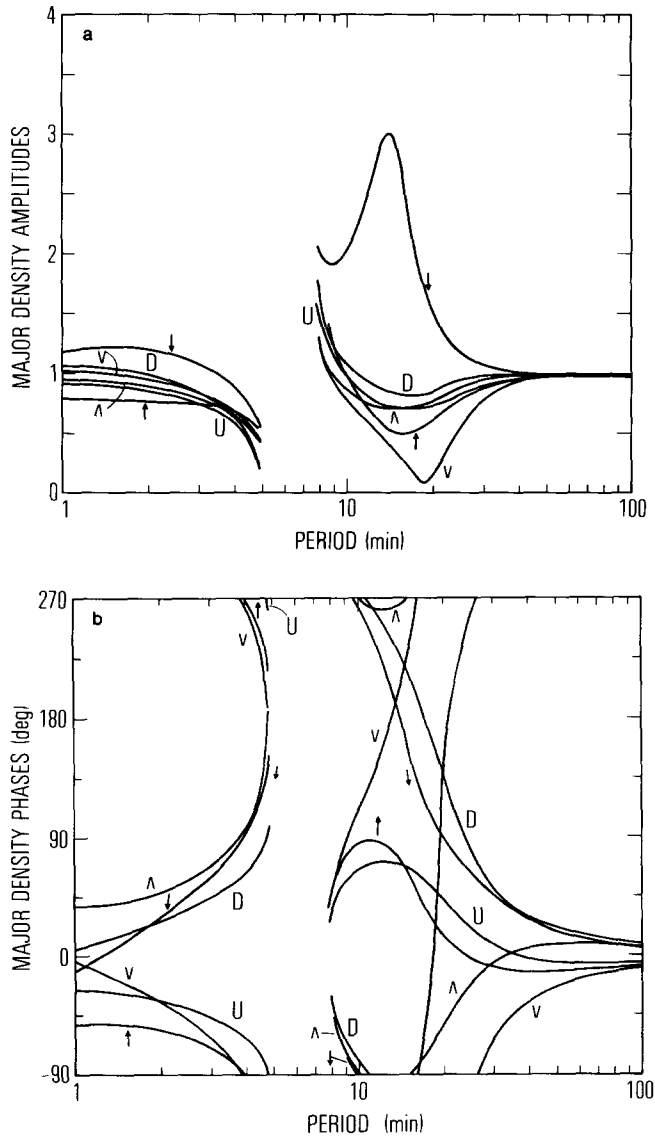


FIG. 5. The same quantities as plotted in the previous figure, but for $\lambda_x = 150$ km at 165-km altitude.

in isolation. However, since the downgoing diffusion mode has an He-CO₂ amplitude ratio of ~ 125 at the near resonance, the observed He-CO₂ ratio should be very large, regardless of the extent to which the diffusion wave is excited by the gravity wave.

The resonance is very localized, as can be seen by comparing Figs. 2, 3, and 4, the last of these showing acoustic-gravity amplitude and phase behavior for a 400-km

wave at 175-km altitude. The He-CO₂ amplitude ratio, which is > 10 at its peak at 154 km, is a factor of 5 lower at both 150- and 175-km altitude. This localization occurs because the vertical wave number for diffusion waves varies approximately as $D_{st}^{-1/2}$, which changes sharply with altitude. Another feature of Fig. 4 is that acoustic properties at the 175-km level are much more variable than at lower levels. This is due to the long collision times at 175 km, and it

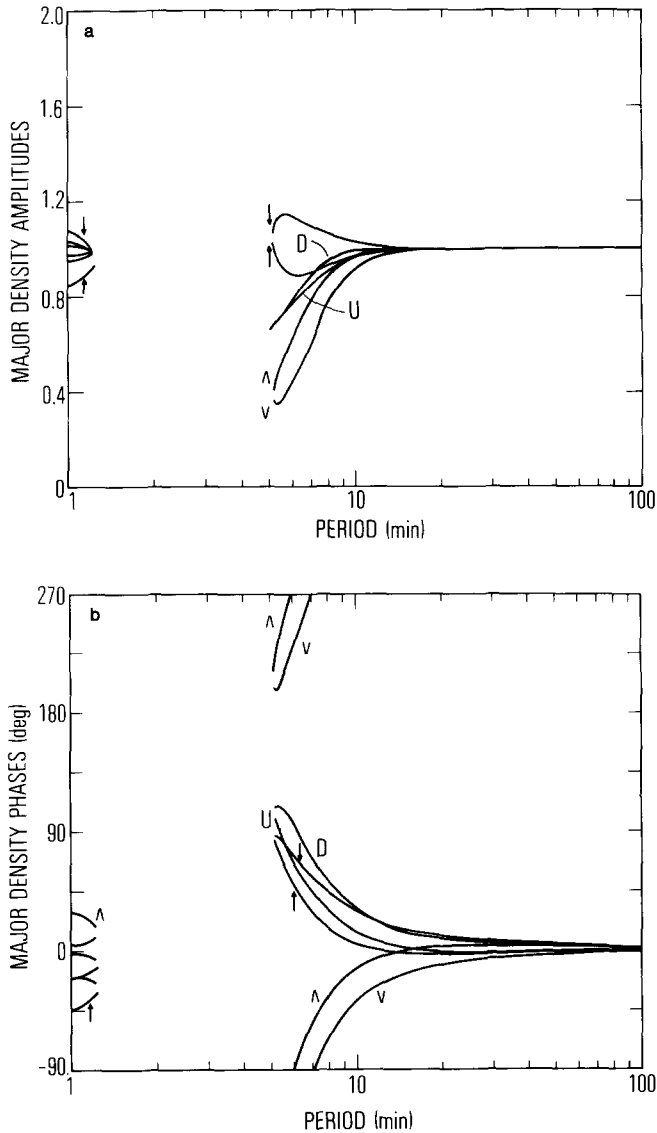


FIG. 6. The same quantities as plotted in the previous figure, but for $\lambda_x = 25$ km at 165-km altitude.

suggests that continuum theory is breaking down.

It is also interesting to see how wave properties vary with horizontal wavelength. Figures 5 and 6 are the results for waves with $\lambda_x = 150$ and 25 km, respectively, at 165-km altitude. In most respects Fig. 5 is very similar to Fig. 3, since horizontal diffusion (which depends on λ_x) is unimportant in the Venus thermosphere except at very

small scale sizes. The one major difference is that once again, the He-CO₂ peak is substantially smaller. In other words, the resonance is highly localized in both altitude and horizontal wavelength. In this case, the localization occurs because internal gravity wave vertical wavelengths vary almost linearly with λ_x , while diffusion waves are only weakly dependent on λ_x except at very small scales. Figure 6, on the other hand, is

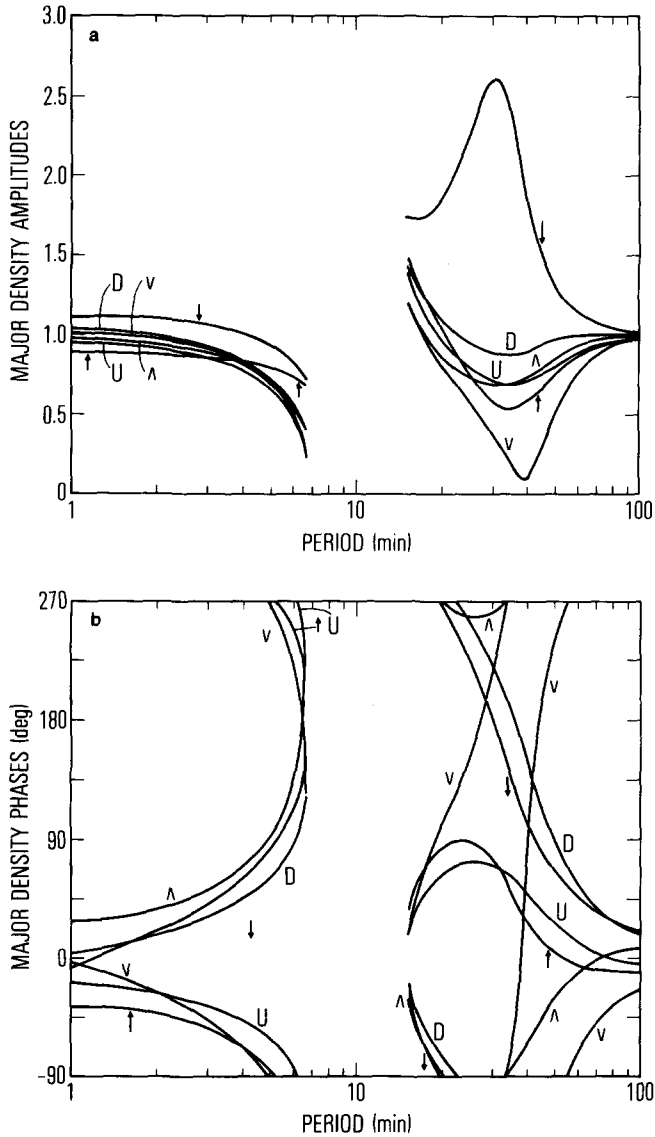


FIG. 7. The same quantities as plotted in Fig. 3, but for a basic state with an exospheric temperature of 650°K.

quite different from the previous cases. For $\lambda_x = 25$ km, $\tau_{diff}^h < \tau_{diff}^v$, and the relevant diffusion time scale is thus τ_{diff}^h . Horizontal diffusion eliminates amplitude and phase differences at all but the shortest internal gravity wave periods, and even at these periods, differences are not as drastic as they are for longer horizontal wavelengths.

Finally, since there is uncertainty about

the dayside exospheric temperature on Venus, we have considered another basic state model to test the sensitivity of our results to the details of background density and temperature profiles. Figure 7 presents the results for the same case as in Fig. 3, but based on the upper atmospheric model of Herman (1973), which assumes a dayside exospheric temperature of 650°K. Except

for the downgoing He-CO₂ amplitude ratio, the two figures are qualitatively similar. This insensitivity to the details of the basic state is encouraging, given our present poor state of knowledge about the upper atmosphere. However, once again, the He-CO₂ resonance peak greatly diminishes when the conditions of Fig. 3 are changed. In this case, the relative absence of resonance for the 650°K exosphere occurs for the following reason. For diffusion waves, the real and imaginary parts of the vertical wavenumber are usually approximately equal in magnitude, but different in sign (Del Genio *et al.*, 1978), so the real part of the vertical wavenumber is also about the same as it was before for the diffusion wave. For internal gravity waves, though, this quantity is approximately $\frac{1}{2}H_p$ and thus varies inversely with the temperature. Consequently, it is reduced by almost a factor of two when the higher exospheric temperature is used, and this is enough to eliminate much of the resonance effect.

ENERGETICS AND DISSIPATION OF WAVE ENERGY

An important aspect of wave-induced diffusion between two atmospheric gases is the resulting dissipation of energy in the direction of the wave's group (i.e., energy) propagation. Damping of wave energy takes place whenever velocity and/or temperature differences between species exist. The phase lag due to the finite time required to smooth out these differences causes a destructive interference between the motions of the two colliding gases, dissipating the wave energy into disorganized thermal energy. Maximum velocity and temperature differences, and hence maximum damping, occur at wave periods comparable to the mean collision and diffusion times, because at these two time scales the disruptions of thermodynamic and diffusive equilibrium, respectively, caused by the wave perturbation do not have sufficient time to be smoothed out before a wave cycle is completed.

In order to estimate the extent of collisional damping in the Venus thermosphere, we need expressions for the total wave energy and the dissipation rate due to wave-induced diffusion. These can be obtained by deriving a total energy conservation equation for the two-fluid system. Del Genio *et al.* (1979) derived such an equation, using the same type of procedure originally employed by Eckart (1960) for non-dissipative acoustic-gravity waves. The total wave energy E is identical in form to that derived by Eckart, but with twice as many terms because of the presence of two gases. The diffusive dissipation rate D takes the form

$$D = K_{st}\{(u'_s - u'_t)^2 + (w'_s - w'_t)^2 + [3k/(m_s + m_t)\bar{T}](T'_s - T'_t)^2\}. \quad (2)$$

In this expression, u and w are the horizontal and vertical velocities, respectively, T is temperature, m is molecular mass, and k is Boltzmann's constant. The subscripts s and t refer to the two gases, primes denote perturbation quantities, and an overbar denotes the basic state. K_{st} , the collision parameter, is equal to the density of either gas times its collision frequency with the other gas.

The significance of this dissipation in the Venus thermosphere can be estimated as follows. We average E and D over one wave cycle of period τ_{wave} ; the fractional energy loss per cycle due to diffusion, in effect a $1/Q$ for the perturbed fluid, can then be expressed as

$$1/Q = \langle D \rangle \tau_{\text{wave}} / \langle E \rangle, \quad (3)$$

where $\langle \rangle$ denotes the cycle average. This approach was also used by Hines (1960) in connection with the viscous damping of terrestrial waves.

Figure 8 is a plot of $1/Q$ vs wave period for acoustic-gravity waves in the O-CO₂ model with $\lambda_x = 400$ km at 165-km altitude on Venus. Dissipation by interspecies collisions is seen to be most important at pe-

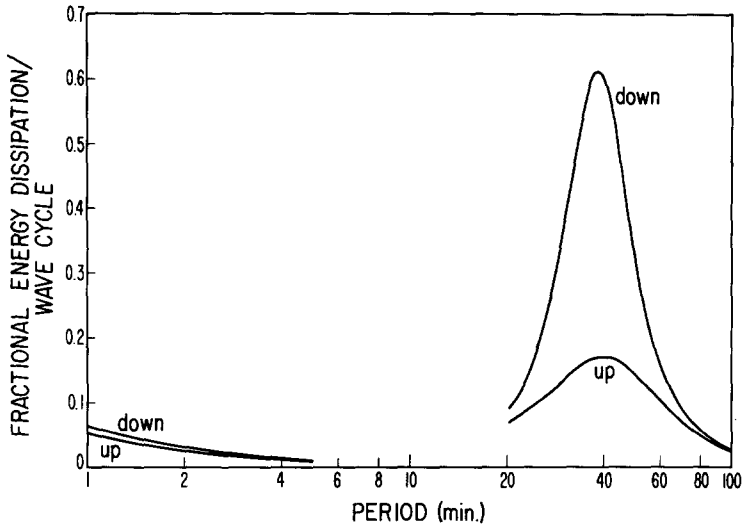


FIG. 8. Fractional energy dissipation over one wave cycle ($1/Q$) as a function of wave period for acoustic-gravity waves with $\lambda_x = 400$ km at 165-km altitude on Venus.

riods comparable to τ_{diff}^v , as expected. The difference between the peak dissipation rates for upgoing and downgoing waves is somewhat surprising; it is probably also a consequence of the vertical anisotropy introduced by the diffusion process. For downgoing waves, at least, dissipation is strong at periods near τ_{diff}^v ; waves at these periods should thus be appreciably damped out after a few wave cycles and would probably not be observed at all except close to their source region. The slight increase in dissipation at the short-period end of Fig. 8 reflects the fact that these periods are approaching the mean O-CO₂ collision time at this altitude.

One difference between dissipation caused by diffusion and other dissipation mechanisms like viscosity and heat conduction is that the strength of damping by diffusion depends on the relative concentrations of the gases. Therefore, while viscous and thermal damping increase monotonically with height in any upper atmosphere, diffusive dissipation will maximize at levels with no single dominant species. This is why only O-CO₂ dissipation is considered here; N₂, CO₂, and He also diffuse rapidly at

165-km altitude, but their low abundances relative to O at this level make them energetically insignificant. Because of the sharp change in composition of the Venus thermosphere with altitude, this also means that dissipation rates will vary sharply with altitude. At 150-km altitude, for example, CO₂ is so much more abundant than any other species that diffusive damping is insignificant at all periods—the maximum $1/Q$ for O-CO₂, which occurs at 82 min period, is only 6.4%. A similar rate would be expected for CO-CO₂ damping, since CO and O are of roughly equal abundance at 150 km in the Kumar and Hunten (1974) model.

At 175 km, on the other hand, CO₂ is only about three times as abundant as O; this, combined with the higher diffusion coefficient at this altitude, results in increased dissipation. Figure 9 shows $1/Q$ vs period for acoustic-gravity waves with $\lambda_x = 400$ km at 175-km altitude. At all periods dissipation is greater than at 165 km. Short-period upgoing internal gravity waves are now severely dissipated, while the corresponding downgoing waves are more or less completely damped out in one cycle

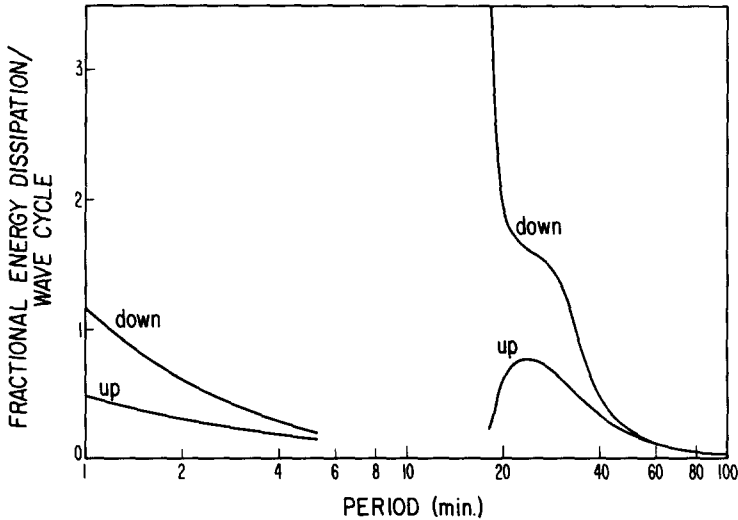


FIG. 9. The same as the previous figure, but at 175-km altitude on Venus.

($1/Q > 1$). At even higher altitudes, with O becoming equal in abundance to CO_2 , D_{st} increasing still further, and He also becoming a major species, we would expect all wave energy to get dissipated over a very short distance.

DISCUSSION

The frequency dependence of dissipation has important implications for Pioneer Venus observations. For periods $\approx \tau_{diff}^v$, dissipation is small, and these waves should be able to propagate far from their sources and still be observed. Waves with periods comparable to τ_{diff}^v , on the other hand, will be strongly damped and should be unobservable except near the source region. At longer periods, even though diffusive dissipation decreases, viscous, thermal, and ionic dissipation should be important, and these waves should also be, for the most part, unobservable. This last point applies, of course, only to medium-scale waves; planetary-scale waves do not dissipate as severely under the influence of viscosity and heat conduction because the velocity and temperature gradients associated with the waves decrease with increasing horizontal scale.

Since the transition from significant am-

plitude and phase differences to zero differences occurs at periods near τ_{diff}^v , and since viscous and heat conduction time scales should be similar to τ_{diff}^v , most waves observed by ONMS should exhibit differential amplitude and phase behavior. However, if long-period waves are generated near the point of observation, they will not yet have dissipated, and we might then expect to see all species oscillations in phase with each other and of equal amplitude. In other words, the presence or absence of amplitude and phase differences is a rough indicator of the proximity of the wave source and it might therefore be possible to use the ONMS wave observations to help map the spatial distribution of heat and momentum sources in the Venus thermosphere.

The differences between He- CO_2 amplitude ratios for upgoing and downgoing waves in our solutions may also prove useful as a means of identification. If the primary solar energy deposition level is below ~ 150 -km altitude, we should observe mostly waves with upward energy propagation in the 150- to 175-km altitude range. For internal gravity waves, this implies downgoing phase, the signature of which should be a large He amplitude relative to the other gases due to the near gravity

wave-diffusion wave resonance. If energy is deposited above the 175-km level, though, we would observe phase propagating upward at lower levels, signifying downward energy propagation and this would be marked by He amplitudes comparable to or less than those of CO₂. Thus, the detection of He oscillations can help determine the altitudes at which thermospheric heating is taking place if that heating generates wave motions.

Of course, both types of sources might exist. The solar euv heating profile on Venus probably deposits the bulk of the heating at the lower levels due to the increasing density with decreasing altitude. Tropospheric and stratospheric (i.e., cloud layer) sources might also supply waves with upward energy flow; in fact, it might be possible to verify this on occasion by comparing ONMS detections of density oscillations with simultaneous observations of wavelike ultraviolet contrasts at the cloud tops by the cloud photopolarimeter (Colin and Hunten, 1977) on the Pioneer Venus Orbiter. The solar wind-ionosphere interaction, on the other hand, probably takes place at a much higher level (Bauer *et al.*, 1977) and this might cause downward energy propagation to also be present.

If He amplitudes are ever observed to be not just >1, but in the range 5–10 or greater, it would indicate that conditions were very close to resonance. Not only would this define the wavelength, period, and source region of the wave, it would also indicate an exospheric temperature close to 350°K. If the Venus thermosphere is as variable as the Earth's, a wide range of temperatures may be possible depending on the level of solar activity at a given time. Thus, when resonant conditions are observed, this might be used to provide an occasional check on temperatures inferred from density scale heights.

To summarize, then, the mass spectrometer on the Pioneer Venus Orbiter should be expected to detect the following wave phenomena:

(1) Virtually no medium-scale waves at all at altitudes higher than ~200 km, due to severe dissipation at all periods at these levels;

(2) wave periods ≤ 30 –35 min at lower altitudes in most cases, because of increased damping of waves with longer periods;

(3) small N₂, CO, and O wave amplitudes relative to CO₂, and highly variable phase differences for all species;

(4) comparable He and CO₂ amplitudes if wave sources are above the 150- to 175-km level, and large He amplitudes if sources are below the 150- to 175-km level, due to the influence of a near resonance between gravity and diffusion waves for upward gravity wave energy propagation;

(5) extremely large He amplitudes at times, if the exospheric temperature is close to 350°K, when the conditions for resonance are satisfied almost exactly;

(6) longer-period waves without discernible amplitude and phase differences on occasion when the satellite passes close to a source region, because these waves have not yet propagated far enough to be damped out completely.

The gravity wave energy dissipated by diffusion should appear as heating at the level of dissipation. A rough estimate of the heating rate H might be

$$H = D/\rho c_p = (\gamma - 1) \langle D \rangle / \gamma n k, \quad (4)$$

where c_p is the specific heat at constant pressure for the atmosphere, γ is the ratio of specific heats, and ρ and n are the total mass and number density, respectively. For downgoing waves at the dissipation peak at 165-km altitude, the vertical velocity contribution represents 98% of the total diffusion dissipation, so

$$\begin{aligned} \langle D \rangle &\approx K_{st} \langle (w'_t - w'_s)^2 \rangle \\ &\approx K_{st} |(w'_t/w'_s - 1)^2 w'^2_s|. \end{aligned} \quad (5)$$

At 39 min period, w'_t and w'_s are <1° out of phase, and $w'_t/w'_s \sim 2$ for O–CO₂. If we assume a wave amplitude of $w'_s \sim 1$ m sec⁻¹, the resulting heating rate is $\sim 4^\circ\text{K day}^{-1}$. A

somewhat more optimistic estimate of wave amplitudes, say $w'_s \sim 5 \text{ m sec}^{-1}$, gives $H \sim 100^\circ\text{K day}^{-1}$. External heating rates on Venus are somewhat uncertain, but it seems possible from this estimate that dissipation of gravity wave energy may represent an important energy source itself for certain parts of the Venus thermosphere. For example, heating in the subsolar region by euV radiation and perhaps by a direct solar wind-ionosphere interaction should be large, and gravity waves might be expected to propagate primarily away from this region toward larger solar zenith angles. Thus, gravity wave energy transport to the nightside of Venus and subsequent dissipation there may be an important heating mechanism on the nightside above the turbopause.

Finally, we note that amplitude and phase differences between species do not necessarily depend on the existence of diffusive equilibrium in the atmosphere. Even below the turbopause, where an atmosphere is generally well mixed, sharply defined layers of various individual gases usually exist due to photochemical or latent heat processes. Such layers do not share the scale height of the background atmosphere and will therefore exhibit amplitude and phase differences relative to the background when a wave passes through. Chiu and Ching (1978), in fact, were able to explain observations of large fluctuations in the terrestrial ozone and sporadic-E layers in this manner. The density amplitude ratio is given by

$$\frac{\rho'_c}{\bar{\rho}_c} = [-1/(\gamma - 1)](1 + \gamma H/L)(\rho'/\bar{\rho}), \quad (6)$$

where $\rho'_c/\bar{\rho}_c$ and $\rho'/\bar{\rho}$ are the fractional layer and background density perturbations, respectively, H is the background scale height, and $L = (\rho_c^{-1}d\rho_c/dz)^{-1}$ is a characteristic length scale for the layer density gradient. For $L = -H_c$, (6) gives the long-period limiting behavior of a diffusively separated atmosphere without wave-

induced diffusion evident in Fig. 1 (Dudis and Reber, 1976).

This could be important in the Venus stratosphere, especially in the cloud region, where several species are probably distributed unevenly with altitude. For example, the visible clouds are believed to have a scale height $\sim \frac{1}{2}$ that of the background CO_2 atmosphere (Lacis, 1975). If certain gaseous species relevant to cloud formation (H_2SO_4 , S, SO_2 , COS, etc.) share this scale height, their fluctuations during wave passage might be 4–5 times as great as the CO_2 wave amplitude. The same result would apply for planetary-scale waves as well as localized gravity waves. For a typical CO_2 wave density perturbation of 10%, the corresponding cloud layer species fluctuations would then be 40–50% of the ambient density of these species. These sharp fluctuations could greatly enhance or suppress the visibility or perhaps even the formation rate of the dark uv clouds (Travis, 1975) over different parts of the wave cycle, by virtue of the preferential advection of large amounts of dark cloud-forming material up to the visible cloud tops over one-half of each cycle. This might help explain why such well-defined wavelike uv contrast features are observed on Venus (Belton *et al.*, 1976). It would be interesting to see whether the Pioneer Venus large-probe mass spectrometer (Colin and Hunten, 1977) detected any such sharp wavelike density fluctuations during its descent through the visible cloud layer of Venus.

ACKNOWLEDGMENTS

This research was supported by NASA under NSG 7164 and by the Aerospace-Sponsored Research Program. We wish to thank Gary Murdock and Jacob Bridger for their assistance in plotting the curves used in this study.

REFERENCES

- BAUER, S. J., BRACE, L. H., HUNTEN, D. M., INTRILIGATOR, D. S., KNUDSEN, W. C., NAGY, A. F., RUSSELL, C. T., SCARF, F. L., AND WOLFE, J. H. (1977). The Venus ionosphere and solar wind interaction. *Space Sci. Rev.* 20, 413–430.

- BELTON, M. J. S., SMITH, G. R., SCHUBERT, G., AND DEL GENIO, A. D. (1976). Cloud patterns, waves and convection in the Venus atmosphere. *J. Atmos. Sci.* **33**, 1394-1417.
- BROADFOOT, A. L., KUMAR, S., BELTON, M. J. S., AND MCELROY, M. B. (1974). Ultraviolet observations of Venus from Mariner 10: Preliminary results. *Science* **183**, 1315-1318.
- CHIU, Y. T., AND CHING, B. K. (1978). The response of atmospheric and lower ionospheric layer structures to gravity waves. *Geophys. Res. Lett.* **5**, 529-542.
- COLIN, L., AND HUNTEN, D. M. (1977). Pioneer Venus experiment descriptions. *Space Sci. Rev.* **20**, 451-525.
- DEL GENIO, A. D., SCHUBERT, G., AND STRAUS, J. M. (1979). Characteristics of acoustic-gravity waves in a diffusively separated atmosphere. *J. Geophys. Res.*, **84**, 1865-1879.
- DEL GENIO, A. D., STRAUS, J. M., AND SCHUBERT, G. (1978). Effects of wave-induced diffusion on thermospheric acoustic-gravity waves. *Geophys. Res. Lett.* **5**, 265-267.
- DICKINSON, R. E., AND RIDLEY, E. C. (1977). Venus mesosphere and thermosphere temperature structure. II. Day-night variations. *Icarus* **30**, 163-178.
- DUDIS, J. J., AND REBER, C. A. (1976). Composition effects in thermospheric gravity waves. *Geophys. Res. Lett.* **3**, 727-730.
- ECKART, C. (1960). *Hydrodynamics of Oceans and Atmospheres*. Pergamon, New York.
- GOSSARD, E. E., AND HOOKE, W. H. (1975). *Waves in the Atmosphere*. Elsevier, Amsterdam.
- GROSS, S. H., AND EUN, H. (1976). Traveling neutral disturbances. *Geophys. Res. Lett.* **3**, 257-260.
- HERMAN, J. R. (1973). Helium in the topside Venus ionosphere. *J. Geophys. Res.* **78**, 4669-4673.
- HINES, C. O. (1960). Internal atmospheric gravity waves at ionospheric heights. *Canad. J. Phys.* **38**, 1441-1481.
- KUMAR, S., AND BROADFOOT, A. L. (1975). He 584 Å airglow emission from Venus: Mariner 10 observations. *Geophys. Res. Lett.* **2**, 357-360.
- KUMAR, S., AND HUNTEN, D. M. (1974). Venus: An ionospheric model with an exospheric temperature of 350°K. *J. Geophys. Res.* **79**, 2529-2532.
- LACIS, A. A. (1975). Cloud structure and heating rates in the atmosphere of Venus. *J. Atmos. Sci.* **32**, 1107-1124.
- MASON, E. A., AND MARRERO, T. R. (1970). The diffusion of atoms and molecules. *Advan. Atom. Molec. Phys.* **6**, 155-232.
- MCELROY, M. B. (1969). The structure of the Venus and Mars atmospheres. *J. Geophys. Res.* **74**, 29-41.
- NIEMANN, H. B., HARTLE, R. E., KASPRZAK, W. T., SPENCER, N. W., HUNTEN, D. M., AND CARIGNAN, G. R. (1979). Venus upper atmosphere neutral composition: Preliminary results from the Pioneer Venus Orbiter. *Science* **203**, 770-772.
- POTTER, W. E., KAYSER, D. C., AND MAUERSBERGER, K. (1976). Direct measurements of neutral wave characteristics in the thermosphere. *J. Geophys. Res.* **81**, 671-676.
- REBER, C. A., HEDIN, A. E., PELZ, D. T., POTTER, W. E., AND BRACE, L. H. (1975). Phase and amplitude relationships of wave structure observed in the lower thermosphere. *J. Geophys. Res.* **80**, 4576-4580.
- RUSSELL, C. T., ELPHIC, R. C., AND SLAVIN, J. A. (1979). Initial Pioneer Venus magnetic field results: Dayside observations. *Science* **203**, 745-748.
- TRAVIS, L. D. (1975). On the origin of ultraviolet contrasts on Venus. *J. Atmos. Sci.* **32**, 1190-1200.
- VON ZAHN, U., KRANKOWSKY, D., MAUERSBERGER, K., NIER, A. O., AND HUNTEN, D. M. (1979). Venus thermosphere: *In situ* composition measurements, the temperature profile, and the homopause altitude. *Science* **203**, 768-770.